

Additional file 1

Contents

1	Bland-Altman diagrams of navicular height and width at foot strike	2
2	Bland-Altman diagrams of minimum navicular height and maximum navicular width	3
3	Bland-Altman diagrams from time points of minimum navicular height and maximum navicular width	4

1 Bland-Altman diagrams of navicular height and width at foot strike

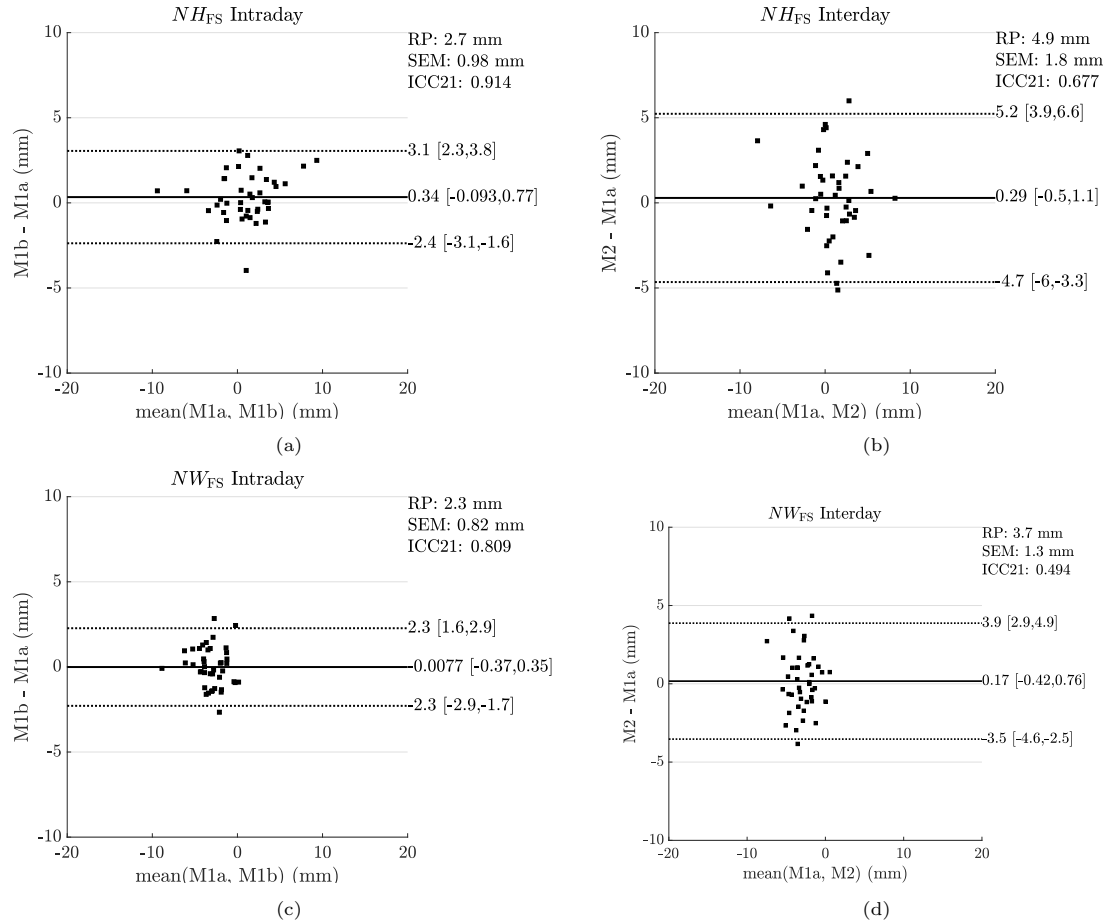


Figure 1: Bland-Altman diagrams with *SEM* and *ICC*₂₁ for intra- and interday reliability of navicular height (*NH*_{FS}) (a) (b) and width (*NW*_{FS}) (c) (d) at foot strike. *RP* denotes the repeatability calculated as $1.96 \times SDd$ (standard deviation of the differences). Solid black lines: bias; Dotted lines: limits of agreement (LoA) calculated as bias $\pm RP$; Numbers in brackets: 95% confidence intervals of bias and LoAs, respectively.

2 Bland-Altman diagrams of minimum navicular height and maximum navicular width

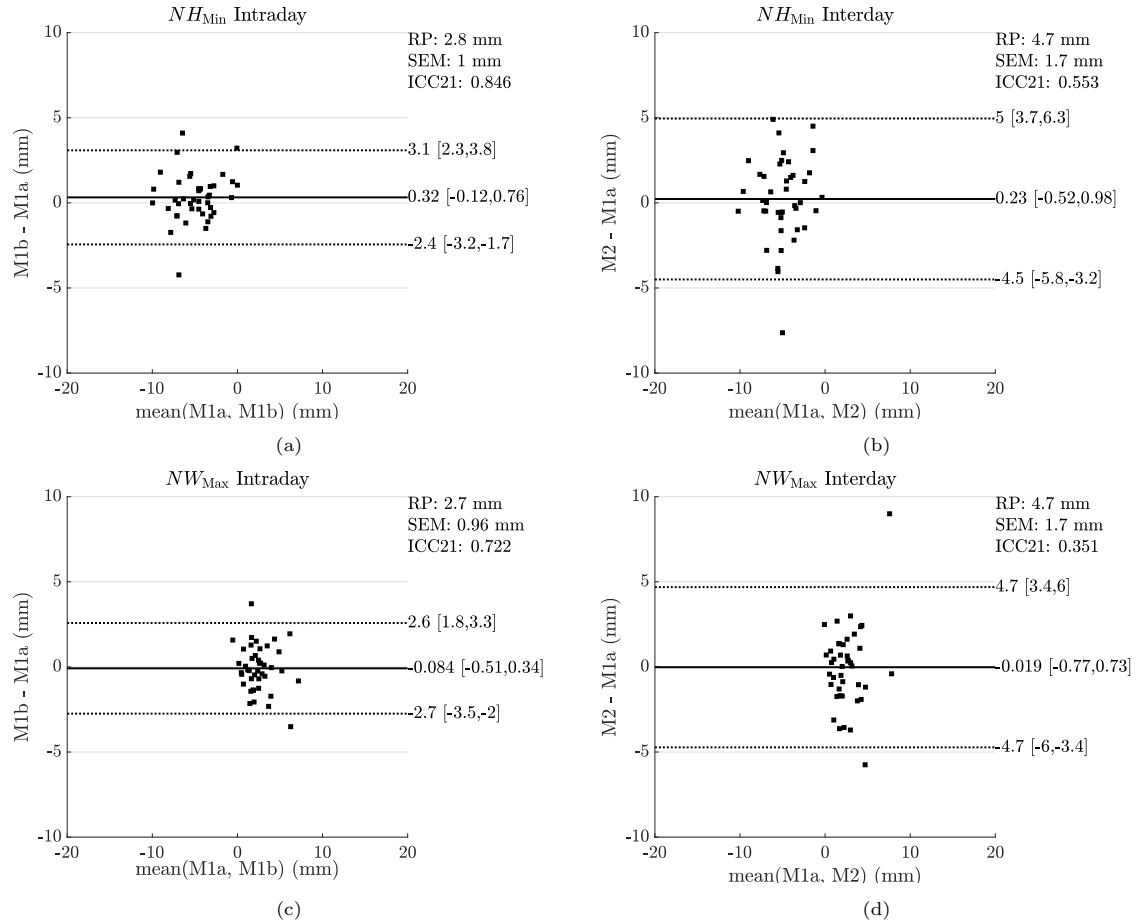


Figure 2: Bland-Altman diagrams with SEM and ICC_{21} for intra- and interday reliability of minimum navicular height (NH_{Min}) (a) (b) and maximum navicular width (NW_{Max}) (c) (d) during the stance phase. RP denotes the repeatability calculated as $1.96 \times SDd$ (standard deviation of the differences). Solid black lines: bias; Dotted lines: limits of agreement (LoA) calculated as bias $\pm RP$; Numbers in brackets: 95% confidence intervals of bias and LoAs, respectively.

3 Bland-Altman diagrams from time points of minimum navicular height and maximum navicular width

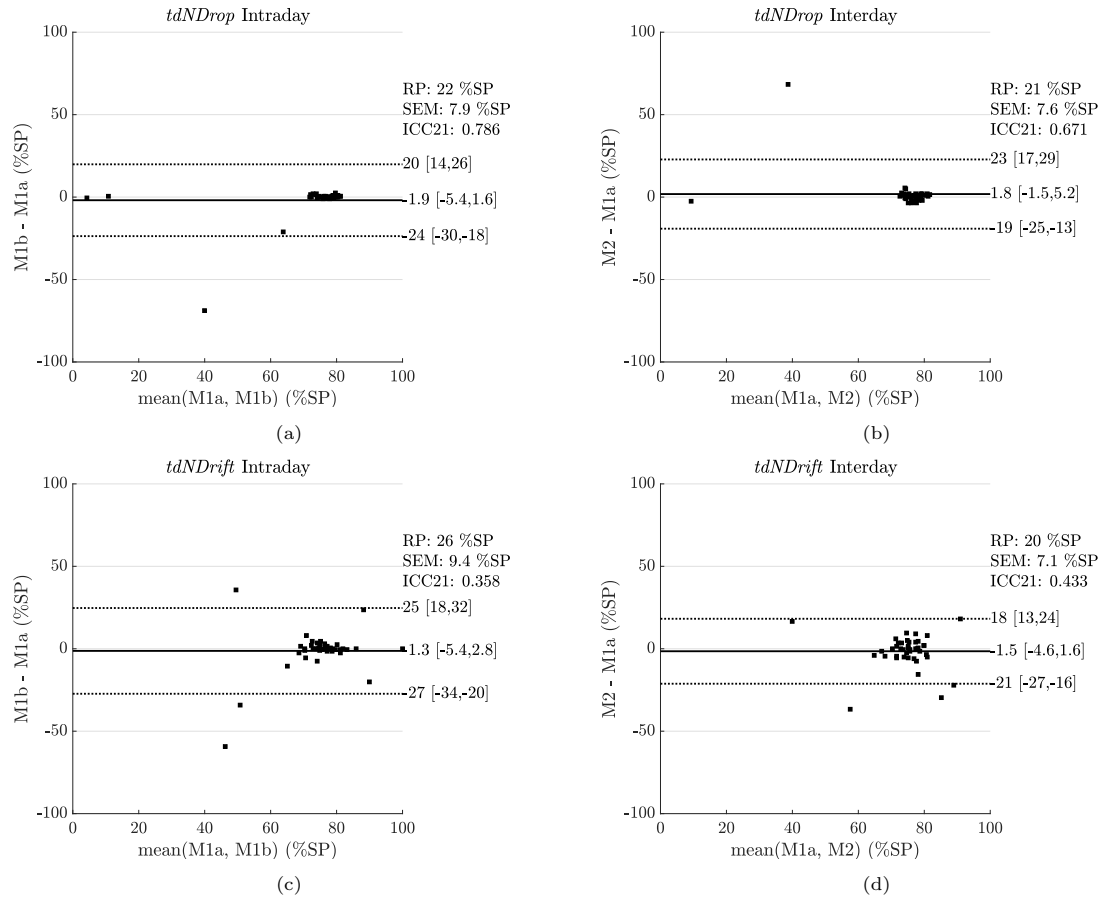


Figure 3: Bland-Altman diagrams with *SEM* and *ICC*₂₁ for intra- and interday reliability of the time points of dynamic navicular drop (*tdNDrop*) (a) (b) and drift (*tdNDrift*) (c) (d) during the stance phase. *RP* denotes the repeatability calculated as $1.96 \times SDd$ (standard deviation of the differences). Solid black lines: bias; Dotted lines: limits of agreement (LoA) calculated as bias $\pm RP$; Numbers in brackets: 95% confidence intervals of bias and LoAs, respectively.